Bioconjugate Chemistry

Article

pubs.acs.org/bc

Imaging Cell Surface Glycosylation in Vivo Using "Double Click" Chemistry

André A. Neves,[†,‡,§] Henning Stöckmann,[†,#,§] Yelena A. Wainman,[†,#] Joe C-H. Kuo,[†] Sarah Fawcett,[†] Finian J. Leeper,[#] and Kevin M. Brindle*[,†,‡]

[†]Cancer Research U.K., Cambridge Institute, Li Ka Shing Centre, Robinson Way, Cambridge CB2 0RE, U.K.

[#]Department of Chemistry, University of Cambridge, Cambridge CB2 1EW, U.K.

[‡]Department of Biochemistry, University of Cambridge, Tennis Court Road, Cambridge CB2 1GA, U.K.

Supporting Information

ABSTRACT: Dynamic alterations in cell surface glycosylation occur in numerous biological processes that involve cell−cell communication and cell migration. We report here imaging of cell surface glycosylation in live mice using double click chemistry. Cell surface glycans were metabolically labeled using peracetylated azido-labeled *N*-acetylgalactosamine and then reacted, in the first click reaction, with either a cyclooctyne, in a Huisgen [3 + 2] cycloaddition, or with a Staudinger phosphine, via Staudinger ligation. The second click reaction was a [4 + 2] inverse electron demand Diels−Alder reaction between a *trans*-cyclooctene and a tetrazine, where the latter reagent had been fluorescently labeled with a far-red fluorophore. After administration of the fluorescent tetrazine, the bifunctional cyclooctyne-cyclooctene produced significant azido sugar-dependent fluorescence labeling of tumor, kidney, liver, spleen, and small intestine in vivo, where the kidney and tumor could be imaged noninvasively in the live mouse.

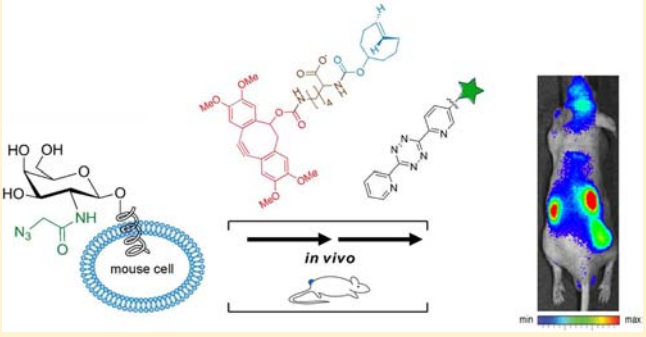

INTRODUCTION

Glycosylation of cell surface proteins is involved in cell differentiation, communication, and migration and is frequently altered in disease, particularly in cancer.[1] Several epithelial tumors overexpress mucin glycoproteins, which can function as scaffolds for various cancer-associated glycan epitopes[2] and are important biomarkers of tumor development, progression and metastasis.[3]

The relative abundance and accessibility of cell surface glycans and their changes in disease have made them attractive targets for noninvasive imaging. Antibodies,[4] peptides,[5] boronic acid-based probes,[6] and lectins[7] have been used for imaging glycosylation in vivo. However, these imaging agents provide only a snapshot view of tissue glycosylation, whereas metabolic labeling with azido-sugars can, in principle, report on the dynamics of glycan turnover. Metabolic labeling with azido-sugars, in conjunction with click chemistry, has been used previously for imaging glycans in mouse tissues, although the click reaction or subsequent imaging was performed ex vivo.[8,9] We reported recently the first demonstration of noninvasive imaging of tumor sialylation in live mice[10] based on labeling of tumor glycans with an azido-sugar, followed by Staudinger ligation with a biotinylated click reagent and subsequent imaging with a fluorescent or radionuclide-labeled avidin probe. Such a pretargeting approach has been widely used previously in radionuclide imaging.[11,12] However, the large size of the avidin, which limited vessel permeability, precluded glycan imaging in normal tissues. The aim of this study was to develop small molecule click reagents that could be used to image azido-sugar labeled glycans in any tissue in the living mouse.

Initially, we produced small molecule click probes, either by direct conjugation of a Staudinger phosphine to a gadolinium chelate, to generate an MRI contrast agent, or by conjugation of a fluorophore to tetramethoxydibenzocyclooctyne (TMDI-BO647),[13] to generate a fluorescent agent. However, the relatively slow reaction rate of azido-labeled sugars with phosphines or cyclooctynes meant that these reagents had to be used at relatively high concentrations, which generated high background signals and failed to give significant contrast in vivo (see Figures S2 and S3 in Supporting Information). Therefore, we developed a two-step labeling strategy ("double-click") in which the first click reagent is a bifunctional reagent, in which a phosphine or cyclooctyne is conjugated to a *trans*-cyclooctene. The imaging probe is then introduced in a second click reaction between the *trans*-cyclooctene moiety and a tetrazine conjugated to the imaging probe (Figure 1). Since this second click reaction is 10^4−10^5 times faster than the first click reaction, between the azido-labeled sugar and the phosphine or

Received: November 22, 2012
Revised: March 24, 2013
Published: May 5, 2013

   dx.doi.org/10.1021/bc300621n | *Bioconjugate Chem.* 2013, 24, 934−941

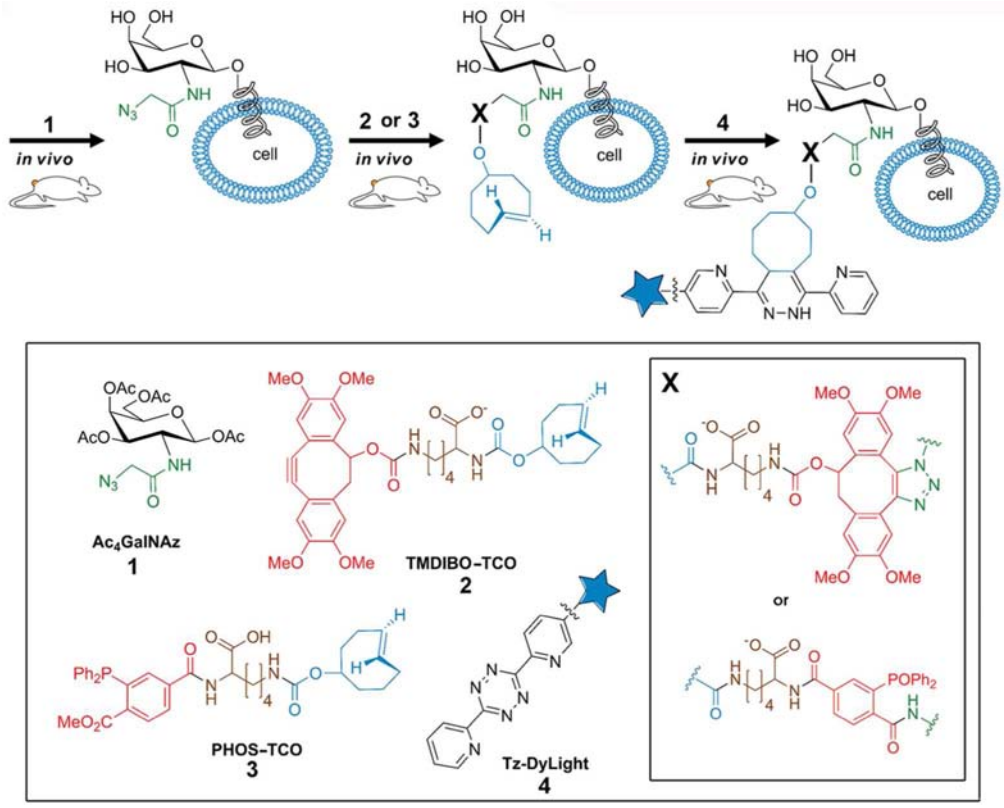

Figure 1. Imaging cell surface glycosylation in vivo. Mice were injected i.p. daily for 3 days with peracetylated azido-labeled *N*-acetylgalactosamine ($Ac_4GalNAz$; **1**), which is incorporated metabolically into *N*-azidoacetylgalactosamine units of cell surface glycans. The azido group in the glycan was reacted in vivo with either TMDIBO-TCO (**2**) or PHOS-TCO (**3**), which were then reacted with Tz-DyLight (**4**) in vivo for subsequent fluorescence imaging.

cyclooctyne, the imaging agent can be used at much lower concentrations. This will lower background and improve image contrast if the nonspecifically bound bifunctional agent is washed out by the time the tetrazine imaging agent is administered or if the *trans*-cyclooctene moiety is inaccessible in the nonspecifically bound form. This strategy has the added advantage that the imaging probe can be used at much lower concentrations, which has a significant cost advantage in the case of the fluorophore-labeled tetrazine and would minimize radiation dose if a radiolabeled agent were used. Similar tetrazine ligations, based on the inverse-electron-demand Diels–Alder reaction, have been used recently for bioconjugation,[14] for modifying live cell surfaces in combination with cyclooctynes,[15,16] although not in vivo, and as single probe in vivo imaging agents.[17]

EXPERIMENTAL PROCEDURES

Cell Culture. Lewis lung carcinoma cells (LL2, from ATCC, Teddington, UK) were grown in complete DMEM medium (Dulbecco's Modified Eagle medium) (Invitrogen, Paisley, UK), supplemented with 10% fetal bovine serum (FBS) (PAA Laboratories, Yeovil, UK) and maintained in 5% CO_2, at 37 °C.

Probe Binding to Serum Albumin. BSA (Sigma-Aldrich, Gillingham, UK) was incubated with either PHOS-TCO (**3**) or TMDIBO-TCO (**2**) (see Figure 1) for 1 h at 37 °C in HBS buffer (20 mM HEPES, 150 mM NaCl, pH 7.40). Tz-DyLight (**4**; Figure 1) was added subsequently and reacted for a further 20 min. The directly conjugated probes, PHOS647, TMDIBO647, and DIFO647[9] were incubated with BSA for 1 h at 37 °C. The mixtures were resolved by native gel electrophoresis (Figure 2; 10% acrylamide, 0.8 M tricine, 1.2 M Tris, pH 8.3 (Expedeon, Harston, UK)). Tz-DyLight fluorescence (excitation, λ: 630 nm; emission, λ: 680 nm) was detected following illumination with 633 nm light using a Typhoon Trio scanner (GE Healthcare, Hatfield, UK). Protein was detected after Coomassie Blue staining (Instant Blue gel stain, Expedeon) using an Image Scanner III scanner (GE Healthcare). Gel densitometry was used to quantitate fluorescence intensity using ImageJ software (National Institutes of Health, Bethesda, MD, USA).

Cell Surface Azido-Glycan Labeling and Flow Cytometry. LL2 cells were incubated for 24 h in complete DMEM medium containing 50 μM of $Ac_4GalNAz$ (**1**; Figure 1) or solvent vehicle (10% DMSO in HBS buffer). The medium was then removed, and the cells were washed with warm PBS and trypsinized (0.25% trypsin, 1 mM EDTA) (Invitrogen) at 37 °C for 5 min. Warm complete DMEM was added to inactivate the trypsin. Cell suspensions were resuspended in cold FACS buffer (1% FBS in HBS buffer) and reacted with TMDIBO-TCO or PHOS-TCO (30 μM in FACS buffer containing 50 nM SYTOX Green (Invitrogen)) for 30 min at 37 °C. Tz-DyLight (20 μM) was then added, and the cells were incubated for a further 20 min. They were then washed three times with cold FACS buffer, filtered through a 50-μm pore-size membrane, and analyzed using a LSRII (BD Biosciences, Oxford, UK) flow cytometer, using 20 000 events. Data analysis was performed using FlowJo software (Tree Star, Ashland, OR, USA). The population of interest (viable cells) was gated based on high levels of NADH autofluorescence and low levels of SYTOX Green staining. The far-red median fluorescence

dx.doi.org/10.1021/bc300621n | *Bioconjugate Chem.* 2013, 24, 934–941

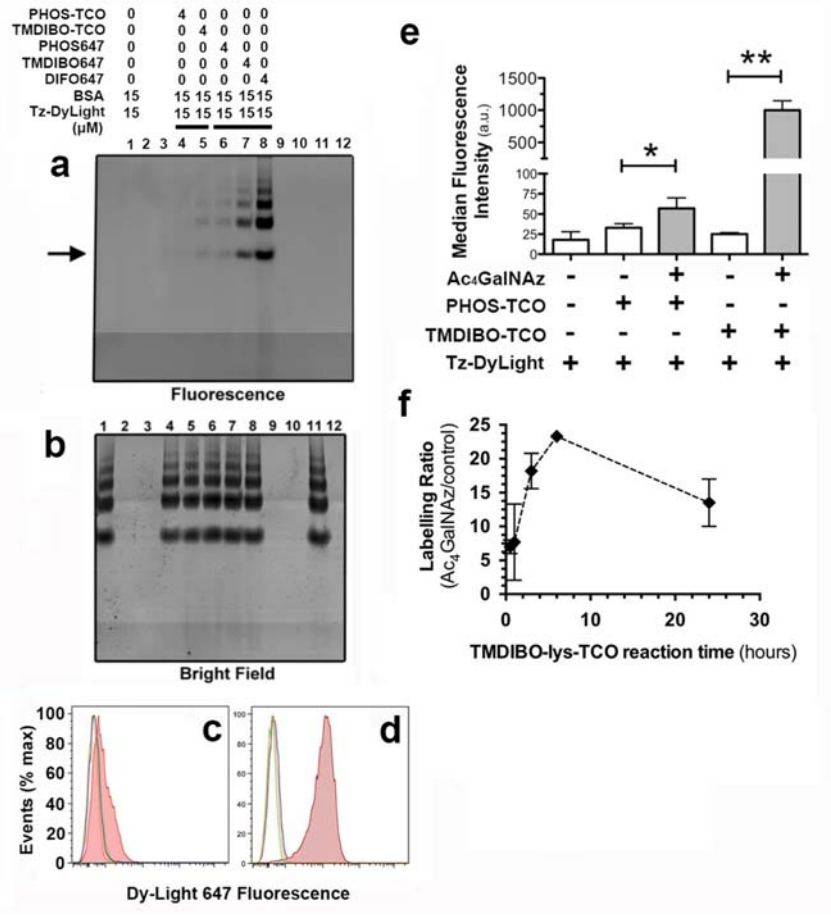

Figure 2. Probe binding to serum albumin (a, b) and flow cytometric analysis of cell labeling (c–f). BSA was incubated with either PHOS-TCO (lane 4, a, b) or TMDIBO-TCO (lane 5, a, b) and the TCO moieties were then reacted with Tz-DyLight. BSA was also incubated with the directly conjugated probes, in which a Staudinger phosphine (PHOS647,[13] lane 6), tetramethoxydibenzocyclooctyne (TMDIBO647,[13] lane 7) or difluorocyclooctyne (DIFO647,[13] lane 8) were directly conjugated to a DyLight647 fluorophore. The BSA in the resulting reaction mixtures was resolved on a native gel and stained with Coomassie Blue. The fluorescence from Tz-DyLight (a) and Coomassie Blue staining (b) were imaged. The BSA monomer is indicated by the black arrow in (a). BSA oligomers frequently form under these conditions. Concentrations (a, b) are expressed in μM. Lanes 2, 3, 9, 10, and 12 were not loaded. Lane 11 contained BSA (15 μM). Lewis lung carcinoma (LL2) cells were cultured in the presence or absence of Ac_4GalNAz for 24 h, washed and then incubated with either PHOS-TCO or TMDIBO-TCO and Tz-DyLight. Fluorescence histograms of cells labeled with PHOS-TCO (c) or TMDIBO-TCO (d). Control groups (cells incubated in the absence of Ac_4GalNAz): green (cells); orange (cells + Tz-DyLight); blue (cells + PHOS-TCO or TMDIBO-TCO + Tz-DyLight); Test group (cells incubated with Ac_4GalNAz): shaded red (cells + Ac_4GalNAz + PHOS-TCO or TMDIBO-TCO + Tz-DyLight). Data in (e) are the mean ± SD (n = 3 replicate experiments/group, *p < 0.05, **p < 0.005). Time course (f) of reaction of TMDIBO-TCO with Ac_4GalNAz labeled LL2 cells.

intensity (MFI) of the viable cell population was then determined. Data points were collected in triplicate.

Tumor Model and Metabolic Labeling in Vivo. BALB/c female nude mice (aged 6–9 weeks) were purchased from Charles River Laboratory (Kent, UK). LL2 cells (5×10^6) were resuspended in ice-cold PBS and implanted (100 μL s.c.) in the lower flank. After 7 days, mice were injected daily i.p. for 3 days with a solution of Ac_4GalNAz (300 mg/kg) in DMSO:PBS (10:90%) or with the solvent vehicle alone. On day 11, TMDIBO-TCO or PHOS-TCO or solvent vehicle (DMSO:PBS, 6.7:93.3% or 0.3:99.7%, respectively) were administered i.p. (67 or 3.3 μmol/kg, respectively). At 3 or 24 h after TMDIBO-TCO administration or 3h after PHOS-TCO administration, Tz-DyLight (0.02 μmol/kg) was administered i.v.

Imaging. Fluorescence imaging was performed using an IVIS-200 camera (Perkin-Elmer, Waltham, MA, USA). Mouse imaging in vivo was performed before and at 6 h, and 24 h after intravenous administration of Tz-DyLight (Figure 3). Image acquisition parameters: emission bandpass filter Cy5.5, excitation filter Cy5.5, epi-illumination, small binning, aperture range F1–F2, exposure 1–2 s; the field of view varied between 19.4 cm (in vivo) and 13.0 cm (ex vivo). All images were normalized by dividing the fluorescence image by a reference illumination image; this resulted in a unit-less fluorescence efficiency scale, which represents the fractional ratio of emitted photons per incident excitation photon, and which was multiplied by a factor of 10^5 for ease of presentation. The excitation and emission band-pass ranges were 615–665 and 695–770 nm, respectively. A far-red background band-pass correction filter (580–610 nm) was also used to subtract autofluorescence.

Probe biodistribution. Tissues were collected at 6 or 24 h after the administration of Tz-DyLight. Tumor, hind limb muscle, skin, kidney, spleen, small intestine, liver, heart, lung and brain were harvested from animals that had been injected with Ac_4GalNAz (or solvent vehicle), TMDIBO-TCO and Tz-DyLight. The tissues were kept briefly at 4 °C, weighed, imaged

dx.doi.org/10.1021/bc300621n | Bioconjugate Chem. 2013, 24, 934–941

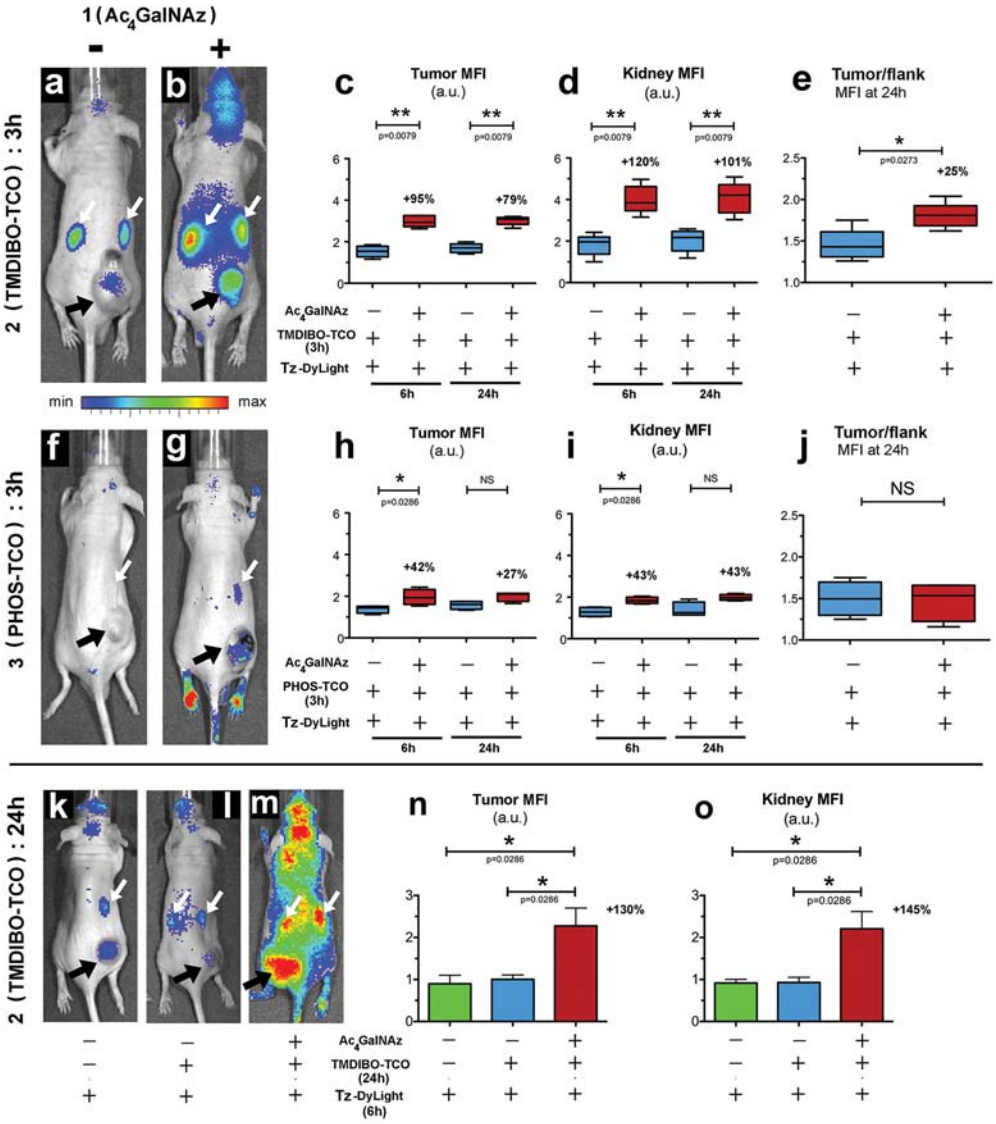

Figure 3. Planar fluorescence images of live mice bearing subcutaneous lung (LL2) tumors, injected i.p. with solvent vehicle (a, f) or $Ac_4GalNAz$ (**1**) (b, g) daily for 3 days and then with TMDIBO-TCO (**2**) (a, b) or PHOS-TCO (**3**) (f, g). The fluorescent imaging agent, Tz-DyLight (**4**), was injected i.v. 3 h (a–j) or 24 h (k-m) after injection of either TMDIBO-TCO or PHOS-TCO. Fluorescence images (λ, excitation: 647 nm; λ, emission: 680 nm) were acquired at 6 and 24 h after the injection of Tz-DyLight. Black and white arrows in (a, b, f–g, k–m) indicate tumors and kidneys, respectively. Data in (c–e, h–j) are mean ± S.E.M., N = 5/group; box plots represent median and 95% confidence intervals. Data shown in (e) and (j) are the ratio of tumor mean fluorescence intensity (MFI) to the adjacent control (flank) tissue MFI at 24 h postinjection of Tz-DyLight. Data in (n–o), in which Tz-DyLight was injected 24 h after injection of TMDIBO-TCO and images were acquired 6 h after injection of Tz-DyLight, are the mean ± S.E.M., N = 3–4/group. Differences were considered significant when $p < 0.05$ (*) or $p < 0.005$ (**).

in the IVIS camera (Figure 4 and S1) and then fixed in neutral buffered formalin (NBF: 4% formaldehyde in PBS) for 24 h, prior to histological analysis. Tissue fluorescence was reported as the ratio of the total fluorescence emission divided by the wet weight of the tissue collected on necropsy, multiplied by a factor of 10^5 for ease of presentation, and reported in arbitrary units (Figures 4 and S1).

Histology and Fluorescence Microscopy. Immediately after collection and fluorescence imaging, tissues were fixed using NBF for 24 h at room temperature and transferred into 70% ethanol before paraffin embedding. Histological sections (8-μm) were dewaxed and stained with either hematoxylin and eosin (H&E) or mounted using aqueous medium (Prolong Gold with DAPI; Invitrogen) for 16 h at room temperature. Slides were then scanned in fluorescence mode (excitation, λ: 633 nm; emission, λ: 680 nm) using a Typhoon Trio scanner (GE Healthcare) at 25-μm resolution.

RESULTS

Cell Labeling and Probe Synthesis. Cell surface glycans were metabolically labeled using **1** (see Figure 1), a peracetylated azido-labeled *N*-acetylgalactosamine ($Ac_4GalNaz$) that is incorporated into the core-0 of mucin-type *O*-linked glycoproteins[18] and also into glycosphingolipids, which are the predominant glycans in lung tumors and in the murine small cell lung cancer cells (LL2) used in this study.[19] The azido-labeled glycans were then reacted, in the first click reaction with **2**, a bifunctional tetramethoxydibenzocyclooctyne conjugated to a *trans*-cyclooctene (TMDIBO-TCO), in a Huisgen [3 + 2] cycloaddition of the azido group with the cyclooctyne, or with

dx.doi.org/10.1021/bc300621n | *Bioconjugate Chem.* 2013, 24, 934–941

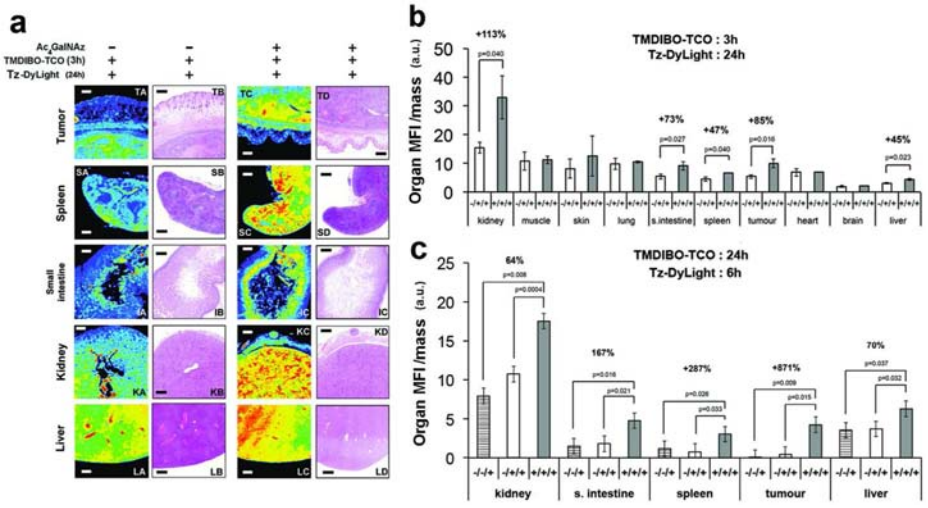

Figure 4. Fluorescence microscopy of metabolically labeled glycans in mouse tissues. Tissues were collected post mortem, fixed for 24 h with 10% formalin and embedded in paraffin. Histological sections were cut, dewaxed, and mounted, and cell nuclei were stained with DAPI. Fluorescence images (columns 1 and 3, from left, in a) were collected at 25-μm resolution and compared with the corresponding H&E-stained sections (columns 2 and 4, from left, in a). The weight-corrected mean whole-organ fluorescence intensities (b, c), calculated from macroscopic images collected using an IVIS 200 camera, are also shown for two panels of mouse tissues (b, c). The times allowed for TMDIBO-TCO and Tz-DyLight clearance from the body, prior to ex vivo imaging, were 3 and 24 h respectively in (b) and 24 and 6 h respectively in (c). Data in (b, c) are mean ± SEM. Differences between groups (b, c) were considered significant when $^*P < 0.05$ ($N = 4–7$/group). Error bars in (b, c) lie within the chart bars when not visible. Scale bars (a): 50 μm.

3, a bifunctional *trans*-cyclooctene-phosphine (PHOS-TCO), via Staudinger ligation of the azido group with the Staudinger phosphine. The *trans*-cyclooctene groups were then reacted, in a very fast[20] second-click reaction involving a [4 + 2] inverse electron demand Diels–Alder reaction, with **4**, a fluorescently labeled tetrazine (labeled with DyLight650; excitation λ: 652 nm; emission λ: 672 nm), whose fluorescence is detectable in surface tissues in vivo. Both TMDIBO-TCO and PHOS-TCO had a negatively charged lysine core to improve aqueous solubility.

Comparison of Probe Binding to Serum Albumin. Molecules, such as TMDIBO-TCO and PHOS-TCO, can bind to serum albumins, removing them from the circulation[21] and conferring upon them the pharmacokinetic behavior of macromolecular agents and thus restricting their tissue access.[13,22] The albumin-binding properties of TMDIBO-TCO and PHOS-TCO were assessed by incubating them with bovine serum albumin (BSA), and subsequently with Tz-DyLight, and then separating the mixture on a native protein gel. BSA was visualized by Coomassie blue staining (Figure 2b) and Tz-DyLight by fluorescence imaging (Figure 2a). BSA shows a characteristic ladder of oligomers on these gels.[13] The BSA-binding profiles were compared with those of TMDIBO (TMDIBO647), a Staudinger phosphine (PHOS647), and a difluorocyclooctyne (DIFO647),[13] in which the fluorophore was conjugated directly to these click reagents. TMDIBO-TCO bound to BSA more strongly than PHOS-TCO (2.6 ± 0.3-fold) (Figure 2) in agreement with previous studies.[13] However, both TMDIBO-TCO and PHOS-TCO showed less BSA-binding (5.0 ± 0.6- and 3.8 ± 0.6-fold less, respectively) than their directly fluorophore-conjugated counterparts (TMDIBO647 and PHOS647) and much less binding than DIFO647.[13] The higher binding of TMDIBO647 and PHOS647 cannot be attributed to the presence of the fluorophore since the same fluorophore was present in Tz-DyLight, which showed no detectable binding to BSA (Figure 2).

Evaluation of Cell Labeling in Vitro. Next, we assessed the reactivity of TMDIBO-TCO and PHOS-TCO for azido-glycan detection in LL2 cells. Cells were cultured in the presence or absence of $Ac_4GalNaz$ for 24 h, washed, and then incubated with either TMDIBO-TCO or PHOS-TCO for 20 min followed by incubation with Tz-DyLight for 20 min. The signal-to-background ratio (SBR) was considerably higher for cells labeled with TMDIBO-TCO than with PHOS-TCO; 40 ± 1 and 1.7 ± 0.4 respectively (Figure 2c–e). These are comparable to SBRs of 23.9 ± 0.8 and 3.3 ± 0.1, obtained when the corresponding probes, in which the fluorophore was attached directly to the phosphine (PHOS647) or cyclooctyne (TMDIBO647),[13] were used, indicating comparable reactivity of the mono- and bifunctional reagents. The time course of the reaction of TMDIBO-TCO with $Ac_4GalNAz$-labeled cells is shown in Figure 2f. $Ac_4GalNAz$-labeled cells or controls were collected at different times following the addition of TMDIBO-TCO, incubated with Tz-DyLight for 20 min, washed and then analyzed by flow cytometry. Cell viability was comparable and >90% in both groups. Reaction of TMDIBO-TCO with the azido-sugar labeled cells increased linearly relative to controls for up to 6 h following addition of TMDIBO-TCO and then plateaued thereafter. The decrease in cell labeling between 6 and 24 h can be explained by cell growth during this period, when the cell number increased by ca. 70%.

Imaging Labeled Glycans in the Living Mouse. Mice bearing subcutaneous LL2 tumors were injected i.p. daily, for three days, with $Ac_4GalNaz$ or with solvent vehicle, and then injected i.p., on day 4, with TMDIBO-TCO or PHOS-TCO and 3 or 24 h later injected i.v. with Tz-DyLight. Fluorescence images were acquired at 6 and 24 h postinjection of Tz-DyLight. There was more fluorescence from the tumors and kidneys of animals injected with $Ac_4GalNaz$ (Figure 3b,g), when compared to controls injected with solvent vehicle (Figure 3a,f), demonstrating glycan-dependent tissue labeling. There was also considerably more fluorescence from these

dx.doi.org/10.1021/bc300621n | *Bioconjugate Chem.* 2013, 24, 934–941

tissues in animals injected with TMDIBO-TCO (>2-fold) when compared to those injected with PHOS-TCO (Figure 3b,g; c,h; d,i). These results were confirmed by ex vivo measurements (Figure 4 and Figure S1). These data are qualitatively in agreement with the differences in LL2 cell labeling observed in vitro (Figure 2c−e). Better labeling with TMDIBO-TCO as compared to PHOS-TCO was confirmed by measurements of the tumor-to-flank fluorescence ratios (Figure 3e,j). These ratios for control animals (injected with solvent vehicle instead of $Ac_4GalNaz$) are a measure of nonspecific probe accumulation in the tumor interstitial space. This tumor-to-flank ratio in vivo, 24 h post injection of the probe was 1.5 ± 0.2 in the animals used here as compared to a much higher value of 2.3 ± 0.4 observed previously with NeutrAvidin as the imaging probe.[10] The lower ratio reflects presumably the much smaller size of the probes compared to NeutrAvidin, which will facilitate their washout, and their lower protein binding when compared to TMDIBO647 (Figure 2). The higher glycan labeling with TMDIBO-TCO as compared to PHOS-TCO (Figure 3) is most likely due to its greater aqueous solubility, which meant that it could be administered at higher concentrations (67 μmol/kg for TMDIBO-TCO versus 3.3 μmol/kg for PHOS-TCO), and also its greater reactivity toward azido-labeled glycans (23.2 ± 1.0-fold; Figure 2e). The fluorescently labeled imaging probe Tz-DyLight was used at 0.02 μmol/kg. Extending the clearance time for TMDIBO-TCO from 3 to 24 h decreased the background fluorescence by ∼50% and thus increased the change in the signal-to-background ratio (Figure 3k−o), from +95% (Figure 3c, 6 h) to +130% (Figure 3n) for tumors and from +120% (Figure 3d, 6 h) to +145% (Figure 3o) for kidneys. In control animals injected with TMDIBO-TCO and Tz-DyLight, in which the TMDIBO-TCO was allowed to clear for only 3 h before injecting the Tz-DyLight, the background was ∼2 au (−/+/+, Figure 3c,d, 6 h), whereas with a clearance time of 24 h the background was ∼1.0 au for both control groups (−/+/+ and −/−/+, Figure 3n,o).

Imaging Tissue Glycans ex Vivo. The limited depth penetration of the fluorescence emission meant that we were only able to image superficial glycan-labeled tissues in vivo (tumor and kidney), however this could easily be extended to deeper tissues by using an imaging modality with greater tissue penetration, such as radionuclide imaging.[10] In order to determine the range of tissues that were labeled we imaged excised tissues at high-resolution (Figure 4a). There was significant labeling of tumor, kidney, small intestine, spleen and liver (Figure 4b,c). Within the tumors, areas rich in tumor cells showed 3.1 ± 0.2-fold greater fluorescent labeling (Figure 4a-TC), whereas areas of dense neutrophil infiltration, which have been reported previously in LL2 tumors and in human non small cell lung carcinoma,[23,24] showed only low levels of fluorescence. Spleen (Figure 4a-SC) showed very intense labeling of the red pulp (12.7 ± 0.7-fold more than control, Figure 4a-SA), which was likely associated with high levels of terminal *N*-acetyl-D-galactosamine residues present in reticulocytes[25] and low labeling of the white pulp, which may reflect the fact that nude mice lack both mature B and T lymphocytes. Small intestine (Figure 4a-IC) showed intense fluorescence located predominantly on the luminal aspect, possibly associated with goblet cells, which are rich in terminal *N*-acetyl-D-galactosamine in cell surface mucins.[26,27] Kidney (Figure 4a-KC) showed an intense renal cortical signal (8.6 ± 0.6-fold more than control, Figure 4b-KA), which may be associated with S3 proximal tubules or collecting ducts, which have high levels of *N*-acetyl-D-galactosamine.[28] Liver (Figure 4a-LC), which is an important site for *N*-acetyl-D-galactosamine protein *O*-glycosylation,[29] showed intense fluorescence (1.6 ± 0.2-fold more than control, Figure 4a-LA) within portal tracts, central vein and in the main hepatic tissue. Brain and heart tissue were unlabeled. Brain glycans have been shown previously not to label with azido-sugars[9] and observation of heart tissue labeling with a different azido-sugar to that used here[10] suggests the failure to detect labeling may be due to limited incorporation of $Ac_4GalNaz$ into heart tissue glycans. A longer TMDIBO-TCO clearance time of 24 h vs 3 h substantially reduced background labeling and thus generated considerably more contrast (10-, 6-, 2.3-, and 1.6-fold more contrast for tumor, spleen, small intestine and liver respectively; see Figure 4b vs 4c). Further work is required to determine the extent to which probe pharmacokinetics and vessel permeability affect the extent of tissue labeling.

DISCUSSION

Click chemistry has been used previously for labeling and imaging cell surface glycans in developing zebrafish[30] and *Caenorhabditis elegans*.[31] In the mouse, tissues including splenocytes, intestine, kidney, heart, and liver have been glycan-labeled. Initially, the click reaction was performed ex vivo, on isolated splenocytes or on protein extracts of the various tissues,[8] and the labeled click reagent was then detected by flow cytometry or Western blotting. Subsequently, the click reactions have been performed in vivo, although detection of azido-labeled glycan that had reacted with the click reagent was again performed ex vivo.[9] Biocompatible, small molecule, and fast-reacting click reagents that can be used to image glycan labeling in vivo in the mouse have yet to be described. We showed previously that we could detect and image azido-sugar labeling of tumor glycans in vivo using a phosphine-biotin probe, in which the biotin was detected, following Staudinger ligation between the azido-sugar and the phosphine, using a NeutrAvidin imaging probe that had been tagged with either fluorescent or radionuclide labels.[10] However, the large size of the NeutrAvidin meant that it could not access normal tissues, and imaging was restricted largely to tumor glycans. The large size of the probe also resulted in relatively high levels of nonspecific tumor retention via the enhanced permeability and retention (EPR) effect.[32] We have since attempted direct conjugation of a Staudinger phosphine to a gadolinium chelate, as a contrast agent for MRI; however, this probe generated a high background signal on MR images acquired in vivo and failed to give significant contrast (Figure S2). A fluorophore-labeled tetramethoxydibenzocyclooctyne (TMDIBO),[13] which has ca. 40-fold faster reactivity with azido-sugar labeled cells in vitro than the Staudinger phosphine,[13] showed ca. 3-fold higher non-azido-sugar dependent retention of the probe in tumors, in comparison with surrounding tissue, at 24 h post injection. This nonspecific tumor retention, which is much higher than that observed with the probes used here (ca. 1.0−1.5-fold; Figure 4), can be explained by its higher protein binding (Figure 2), which again impaired the development of significant contrast in vivo (Figure S3).

We have described here a double click labeling approach for imaging cell surface glycans in mouse tissues in vivo, which employs small molecule reagents that can access normal tissues and which show good clearance properties. In the first bio-orthogonal click reaction, TMDIBO or PHOS groups react

with an azido-labeled sugar that has been incorporated into cell surface glycans, and then, in a second click reaction, the TCO group reacts with a fluorescently labeled tetrazine (Tz-DyLight). We have shown that these reagents will fluorescently label tumor, spleen, kidney, liver, and small intestine in vivo, although only tumor and kidney tissue could be imaged in vivo due to the limited tissue penetration of light in the far-red range. In tumors and kidney, we showed that TMDIBO-TCO was much better at labeling glycans than PHOS-TCO (Figure 4). This is most likely due to its greater aqueous solubility, which means that it can be administered in vivo at higher concentrations, and also its greater reactivity toward azido-labeled glycans (~20-fold; Figure 3). The fluorescently labeled imaging probe, Tz-DyLight, could be used at much lower concentrations since the [4 + 2] Diels–Alder reaction between TCO and tetrazine is very fast (k_2 = 13090 M^{-1} s^{-1} measured in PBS buffer at 37 °C[16]) when compared to the [2 + 3] cycloaddition between the azido-sugar and the TMDIBO (9.4 × 10^{-2} M^{-1} s^{-1} in MeOH).[9] Moreover, reaction of the tetrazine in Tz-Dylight with a TCO group increases the far-red fluorescence of DyLight647, which in the case of TMDIBO-TCO increased by 60% (see Supporting Figures S4 and S5). All three reagents showed relatively low protein binding (Figure 2), which facilitated their clearance from the body and thus produced relatively rapid tissue contrast. In this study, TMDIBO-TCO or PHOS-TCO were administered 3 or 24 h before the Tz-DyLight and the animals were then imaged at 6 and 24 h after Tz-DyLight administration. Increasing the clearance time for the "double click" probe TMDIBO-TCO from 3 to 24 h substantially reduced the background and thus generated considerably more glycan-dependent contrast, both in vivo (Figure 3) and ex vivo (Figures 4 and S1), particularly in tumor tissue, where the contrast was increased by ~40% in vivo and ~10× ex vivo. Image contrast in tumor and kidney, however, was not improved on increasing the clearance time for Tz-DyLight from 6 to 24 h; in fact, there was a slight decrease in image contrast by 24 h (Figure 3).

CONCLUSIONS

In summary, the bifunctional probes described here provide a set of chemical tools with which to image tissue glycosylation in vivo. These probes represent a significant advance over those described previously in that they show much lower levels of nonspecific albumin binding than the corresponding mono-functional probes and also better tissue penetration and lower levels of nonspecific retention in vivo than a macromolecular imaging probe used previously.[10] These characteristics led to glycan-dependent labeling of normal tissues in vivo as well as better image contrast in tumors.

ASSOCIATED CONTENT

Supporting Information

Details of synthesis, spectral data, and data collected with single-click agents in vitro and in vivo. This material is available free of charge via the Internet at http://pubs.acs.org/

AUTHOR INFORMATION

Corresponding Author

*Tel. +44 0-1223 333674. Fax +44 0-1223 766002. E-mail: kmb1001@cam.ac.uk.

Author Contributions

§(A.A.N. and H.S.) Equal contributions.

Notes

The authors declare no competing financial interests.

ACKNOWLEDGMENTS

We thank Jane Gray, Scott Lyons, and Mikko Kettunen for technical assistance. H.S., J.K., and Y.A.W. were in receipt of Cancer Research UK Ph.D. studentships. S.F. was the recipient of a Ph.D. studentship from the Cambridge Biomedical Research Centre of the National Institute of Health Research with financial support from GlaxoSmithKline UK. This work was supported by a Cancer Research UK programme grant to K.M.B.

REFERENCES

(1) Fuster, M. M., and Esko, J. D. (2005) The sweet and sour of cancer: Glycans as novel therapeutic targets. *Nat. Rev. Cancer 5*, 526–542.

(2) Kufe, D. W. (2009) Mucins in cancer: Function, prognosis and therapy. *Nat. Rev. Cancer 9*, 874–885.

(3) Hollingsworth, M. A., and Swanson, B. J. (2004) Mucins in cancer: Protection and control of the cell surface. *Nat. Rev. Cancer 4*, 45–60.

(4) Gold, D. V., Karanjawala, Z., Modrak, D. E., Goldenberg, D. M., and Hruban, R. H. (2007) PAM4-reactive MUC1 is a biomarker for early pancreatic adenocarcinoma. *Clin. Cancer Res. 13*, 7380–7387.

(5) Medarova, Z., Rashkovetsky, L., Pantazopoulos, P., and Moore, A. (2009) Multiparametric monitoring of tumor response to chemotherapy by noninvasive imaging. *Cancer Res. 69*, 1182–1189.

(6) Geninatti Crich, S., Alberti, D., Szabo, I., Aime, S., and Djanashvili, K. (2013) MRI visualization of melanoma cells by targeting overexpressed sialic acid with a Gd(III)-dota-en-pba imaging reporter. *Angew. Chem., Int. Ed. Engl. 52*, 1161–1164.

(7) Bird-Lieberman, E. L., Neves, A. A., Lao-Sirieix, P., O'Donovan, M., Novelli, M., Lovat, L. B., Eng, W. S., Mahal, L. K., Brindle, K. M., and Fitzgerald, R. C. (2012) Molecular imaging using fluorescent lectins permits rapid endoscopic identification of dysplasia in Barrett's esophagus. *Nat. Med. 18*, 315–321.

(8) Prescher, J. A., Dube, D. H., and Bertozzi, C. R. (2004) Chemical remodelling of cell surfaces in living animals. *Nature 430*, 873–877.

(9) Dube, D. H., Prescher, J. A., Quang, C. N., and Bertozzi, C. R. (2006) Probing mucin-type O-linked glycosylation in living animals. *Proc. Natl. Acad. Sci. U. S. A. 103*, 4819–4824.

(10) Neves, A. A., Stöckmann, H., Harmston, R. R., Pryor, H. J., Alam, I. S., Ireland-Zecchini, H., Lewis, D. Y., Lyons, S. K., Leeper, F. J., and Brindle, K. M. (2011) Imaging sialylated tumor cell glycans in vivo. *FASEB J. 25*, 2528–2537.

(11) Goldenberg, D. M., Sharkey, R. M., Paganelli, G., Barbet, J., and Chatal, J. (2006) Antibody Pretargeting Advances Cancer Radioimmunodetection and Radioimmunotherapy. *J. Clin. Oncol. 24*, 823–834.

(12) Cauchon, N., Langlois, R., Rousseau, J. A., Tessier, G., Cadorette, J., Lecomte, R., Hunting, D. J., Pavan, R. A., Zeisler, S. K., and van Lier, J. E. (2007) PET imaging of apoptosis with (64)Cu-labeled streptavidin following pretargeting of phosphatidylserine with biotinylated annexin-V. *Eur. J. Nucl. Med. Mol. Imaging 34*, 247–258.

(13) Stöckmann, H., Neves, A. A., Stairs, S., Ireland-Zecchini, H., and Brindle, K. M. (2011) Development and evaluation of new cyclooctynes for cell surface glycan imaging in cancer cells. *Chem. Sci. 2*, 932–936.

(14) Blackman, M. L., Royzen, M., and Fox, J. M. (2008) Tetrazine Ligation: Fast Bioconjugation Based on Inverse-Electron-Demand Diels-Alder Reactivity. *J. Am. Chem. Soc. 130*, 13518–13519.

(15) Devaraj, N. K., Weissleder, R., and Hilderbrand, S. A. (2008) Tetrazine-Based Cycloadditions: Application to Pretargeted Live Cell Imaging. *Bioconjugate Chem. 19*, 2297–2299.

(16) Peterson, V. M., Castro, C. M., Lee, H., and Weissleder, R. (2012) Orthogonal Amplification of Nanoparticles for Improved Diagnostic Sensing. *ACS Nano 6*, 3506−3513.
(17) Devaraj, N. K., Thurber, G. M., Keliher, E. J., Marinelli, B., and Weissleder, R. (2012) Reactive polymer enables efficient in vivo bioorthogonal chemistry. *Proc. Natl. Acad. Sci. U. S. A. 109*, 4762−4767.
(18) Hang, H. C., Yu, C., Kato, D. L., and Bertozzi, C. R. (2003) A metabolic labeling approach toward proteomic analysis of mucin-type O-linked glycosylation. *Proc. Natl. Acad. Sci. U. S. A. 100*, 14846−14851.
(19) Yu, C. J., Yang, P. C., Shew, J. Y., Hong, T. M., Yang, S. C., Lee, Y. C., Lee, L. N., Luh, K. T., and Wu, C. W. (1996) Mucin mRNA expression in lung adenocarcinoma cell lines and tissues. *Oncology 53*, 118−126.
(20) Rossin, R., Verkerk, P. R., van den Bosch, S. M., Vulders, R. C. M., Verel, I., Lub, J., and Robillard, M. S. (2010) In vivo chemistry for pretargeted tumor imaging in live mice. *Angew. Chem., Int. Ed. 49*, 3375−3378.
(21) Bertucci, C., and Domenici, E. (2002) Reversible and covalent binding of drugs to human serum albumin: Methodological approaches and physiological relevance. *Curr. Med. Chem. 9*, 1463−1481.
(22) Chang, P. V., Prescher, J.a., Sletten, E. M., Baskin, J. M., Miller, I.a., Agard, N. J., Lo, A., and Bertozzi, C. R. (2010) Copper-free click chemistry in living animals. *Proc. Natl. Acad. Sci. U. S. A. 107*, 1821−1826.
(23) Houghton, A. M., Rzymkiewicz, D. M., Ji, H. B., Gregory, A. D., Egea, E. E., Metz, H. E., Stolz, D. B., Land, S. R., Marconcini, L. A., Kliment, C. R., et al. (2010) Neutrophil elastase-mediated degradation of IRS-1 accelerates lung tumor growth. *Nat. Med. 16*, 219−223.
(24) Wislez, M., Fleury-Feith, J., Rabbe, N., Moreau, J., Cesari, D., Milleron, B., Mayaud, C., Antoine, M., Soler, P., and Cadranel, J. (2001) Tumor-derived granulocyte-macrophage colony-stimulating factor and granulocyte colony-stimulating factor prolong the survival of neutrophils infiltrating bronchoalveolar subtype pulmonary adenocarcinoma. *Am. J. Pathol. 159*, 1423−1433.
(25) Reisner, Y., Itzicovitch, L., Meshorer, A., and Sharon, N. (1978) Hemopoietic stem cell transplantation using mouse bone marrow and spleen cells. *Proc. Natl. Acad. Sci. U. S. A. 75*, 2933−2936.
(26) Roth, J. (1984) Cytochemical localization of terminal N-acetyl-D-galactosamine residues in cellular compartments of intestinal goblet cells: Implications for the topology of O-glycosylation. *J. Cell Biol. 98*, 399−406.
(27) Iida, S., Takeuchi, H., Kato, K., Yamamoto, K., and Irimura, T. (2000) Order and maximum incorporation of N-acetyl-D-galactosamine into threonine residues of MUC2 core peptide with microsome fraction of human-colon-carcinoma LS174T cells. *Biochem. J. 347*, 535−542.
(28) Laitinen, L., Virtanen, I., and Saxé, L. (1987) Changes in the glycosylation pattern during embryonic development of mouse kidney as revealed with lectin conjugates. *J. Histochem. Cytochem. 35*, 55−65.
(29) Lee, A., Chick, J. M., Kolarich, D., Haynes, P. A., Robertson, G. R., Tsoli, M., Jankova, L., Clarke, S. J., Packer, N. H., and Baker, M. S. (2011) Liver membrane proteome glycosylation changes in mice bearing an extra-hepatic tumor. *Mol. Cell. Proteomics 10*, M900538MCP200.
(30) Baskin, J. M., Dehnert, K. W., Laughlin, S. T., Amacher, S. L., and Bertozzi, C. R. (2010) Visualizing enveloping layer glycans during zebrafish early embryogenesis. *Proc. Natl. Acad. Sci. U. S. A. 107*, 10360−10365.
(31) Laughlin, S. T., and Bertozzi, C. R. (2009) *In vivo* imaging of *Caenorhabditis elegans* glycans. *ACS Chem. Biol. 4*, 1068−1072.
(32) Maeda, H., Wu, J., Sawa, T., Matsumura, Y., and Hori, K. (2000) Tumor vascular permeability and the EPR effect in macromolecular therapeutics: A review. *J. Controlled Release 65*, 271−284.